**James D. Freels · Prashant K. Jain · Randy W. Hobbs**

# Design and Nuclear-Safety Related Simulations of Bare-Pellet Test Irradiations for the Production of Pu-238 in the High Flux Isotope Reactor using COMSOL

**Abstract** The Oak Ridge National Laboratory (ORNL)is developing technology to re-establish the capability to produce plutonium-238 for the National Aeronautics and Space Administration (NASA) as a power source material for powering vehicles while in deep-space[1]. The High Flux Isotope Reactor (HFIR) of ORNL has been utilized to perform test irradiations of encapsulated neptunium oxide ($NpO_2$) and aluminum powder bare pellets for purposes of understanding the performance of the pellets during irradiation[2]. Post irradiation examinations (PIE) are currently underway to assess the effect of temperature, thermal expansion, swelling due to gas production, fission products, and other phenomena.

**Keywords** nuclear fuel, heat transfer, fluid flow, structural mechanics, COMSOL, thermal expansion, radioisotope, power

## 1 Introduction

In order to properly assess the design and nuclear-safety implications of the $NpO_2$ pellets and capsules used to produce Pu-238, COMSOL v4.2a has recently been qualified to perform nuclear-safety-related calculations at HFIR. The present design and safety analysis simulates the bare-pellet test capsule assembly in full three dimensions (3D) over a quarter slice of the capsule. The simulation fully couples the heat transfer and structural-thermal mechanics physics, and incorporates a best-estimate representation including nonlinear gap conductance modeling. The results show that the design should produce the desired results provided that the proper pellet side gap size is chosen (on the order of 0.001-inch to 0.0025-inch radial gap). The nuclear-safety goal is to demonstrate that the maximum pellet temperature during the entire irradiation cycle will not exceed the pellet melting temperature (taken to be 650 °C). The results shown herein demonstrate that, for the worst cases, credit must be taken for pellet side-gap closure due to thermal expansion in order to sufficiently cool the pellet and prevent melting. Therefore, the model correlations used for gap conductance[3] are vitally important to demonstrate adequate cooling.

The developed COMSOL model includes several features that may be of interest to the COMSOL community of users including: (1) CAD geometry input and subsequent manipulation, (2) mesh design considerations, (3) heat transfer of both solid and fluid, (4) elastic structural mechanics including thermal expansion, (5) application of complex thin-film resistance, (6) feedback upon the gas-gap conductance as a result of the surface pressure created by the thermally-expanding contact pairs upon the pellet surfaces, (7) complex variable and function structure embedded directly into the COMSOL model to create a best-estimate of the gas-gap conductance incorporated into the thin-film resistance, and (8) completely non-linear variable properties including conservative estimates of the pellet properties. The resulting solution is highly nonlinear and difficult to obtain; particularly after the pellet surfaces are pressed against the side walls of the encapsulation.

Research supported by the Department of Energy (DOE) Offices of Science and Nuclear Energy and the National Aeronautics and Space Administration (NASA)

Oak Ridge National Laboratory
1 Bethel Valley Road
P.O. Box 2008
Oak Ridge, TN 37831-6392
Office: (865)576-8645
Fax: (865)241-2712
E-mail: freelsjd@ornl.gov · jainpk@ornl.gov · hobbsrw@ornl.gov

## 2 Geometry Creation and Proper Meshing

The geometry for this analysis was initialized by directly importing a 3D CAD file representation of the geometry. The interfacing program, Microstation[4], was not directly listed as a supported CAD software for COMSOL. The Microstation experience level is high at the HFIR facility (which has operated since 1966), so changing CAD programs to accommodate COMSOL is not feasible. Furthermore, Microstation is now available at ORNL through a site license, so there is no incentive to change at the present time.

A CAD livelink was not necessary for our design process, so a common input format that is generated as an output file from Microstation was readily accepted. Sev-

eral different formats worked properly and were tested, but it was appropriate to utilize the Parasolid format.

The final assembly of parts were readily input into COMSOL from the Parasolid file out of Microstation. After the initial input, there were several steps that were performed before a final geometry was created for the analysis. Perhaps one of the more important steps was the CAD-import kernel provided feature, "cap", where the open ends of the capsule were closed off, much like the actual seal weld that is performed in reality, and an internal fluid volume of helium is created. The resulting helium volume yielded many very-thin regions where thin gaps are designed into the capsule. Early on, it became evident that these thin gaps were not easily meshed with the rest of the geometry. Therefore, additional geometry operations were performed to eliminate these thin regions from the geometry and replace the the thin regions with the thin film approximation (see section 5).

Several additional geometry operations were necessary. There were also helium "rings" created between the adjacent parts in the axial direction that were created by the chamfer design of the cylinder edges. These "rings" caused great difficulty in meshing, so they too were eliminated from the geometry under the assumption of an insulated region. There were also several features where sharp edges, thin surfaces, etc., were cleaned from the CAD geometry using the COMSOL geometry tools available. One final geometry operation was to cut out a $\frac{1}{4}$ pie slice from the total capsule volume along the axial direction. This "pie slice" operation was necessary in order to create a stable boundary condition for the pellet structural mechanics (see section 6). The final geometry could have been assembled cleanly as a union operation, but instead, it was necessary to create an assembly of three final parts due to the requirement for contact surfaces from the moving structural mechanics parts. The three final parts represented (a) the pellet, (b) the lower-half parts around the pellet, and (c) the upper-half parts around the pellet.

The final meshed geometry of the $\frac{1}{4}$ sliced capsule assembly is shown in Fig. 1. The mesh shown is the "coarse" mesh, which represents the third level of meshing investigated for this simulation. Four levels of meshing were investigated, and both a linear and quadratic finite element basis were utilized. It was found that the lowest-level of meshing was sufficient, provided the quadratic finite-element basis shape functions were also utilized for both the heat transfer, and structural mechanic equations being solved.
[1]

It should also be mentioned that due to the nuclear-safety requirements of the analysis, both normal design, and extreme tolerance levels in the geometry were considered in order to arrive at a conservative estimate of maximum temperature in the pellet.

[1] The reader is invited to zoom in on the .pdf form of the figures in this paper to enable detailed viewing.

**Fig. 1** Coarse Mesh of the Entire Capsule from an Internal View.

## 3 Material Properties

Except for the pellet, all the material properties for this model were obtained directly from the COMSOL material library module. The materials in this library are very specific to the individual alloys available for a material type. The capsule housing, end plug, lower heat sink, and flux monitor cap are all made of Al-6061-T6. The upper heat sink is made of pure copper. The spring and screw are made of 304-SS. The fluid volume is initially assumed to be pure helium gas. Degradation in helium thermal conductivity and gas-gap conductance jump condition were conservatively accounted for by the introduction of fission-gas products at the end of the first and second irradiation cycle. Comparison of the utilized properties from the COMSOL material library against other material library property sources also commonly used at ORNL for similar tasks[5] was also performed.

No prior measured information existed for the material properties of the $NpO_2$ pellets, such as thermal conductivity, thermal expansion, etc., which are required to perform the analysis. Therefore, it was necessary to directly measure some properties prior to irradiation, and conservatively estimate the remaining properties based on material expertise available at ORNL and prior experience with fabrication of similar fissile materials. The net result, obtained through this COMSOL simulation, is a very conservative estimate of pellet temperature, while also allowing for a sufficient production of Pu-238 for the customer.

## 4 Thermal-Structure Interaction Physics

The "heat transfer in solids" module is chosen as the base physics employed by the COMSOL model. This module also allows for a fluid to be included as as separate domain within the model since all the domains are coupled. The "linear-elastic structural mechanics" module is also coupled into the physics. The structures are allowed to thermally expand by coupling with the heat transfer equations. The pellet and two large heat sinks around the pellet are

enabled with thermal-expansion physics of the structural mechanics module. The remaining domains are not enabled for thermal expansion since the temperature changes beyond these domains is small by comparison. Contact pairs are defined between the pellet and all the surfaces surrounding the pellet so that the surfaces do not cross the boundaries defined by the respective domains. Surface pressure can be created by the forces caused by the adjacent thermal expansions of the effected materials. The gas gaps in the model beyond the heat sink domains are conservatively held at constant thickness, thus adding to the conservatism in the model.

## 5 Exploiting the Thin-Film Resistance Feature of COMSOL

The contact pairs between the pellet and the adjacent domains allows for an accurate simulation of the gas gaps between these parts. The initial nominal size of the cold gap on the sides of the pellet is between 1 and 2.5 mils (0.001 inches). The cold gas gap size at the top and bottom of the pellet is essentially the mean size of the surface roughness since these surfaces are initially pressed firmly by the spring force designed from the top of the pellet. The purpose of this design feature is to try to allow enough initial gas-gap size to be able to measure the effect of fission-gas expansion of the pellet during the irradiation cycle. At the same time, the gas gap must not be so large that is causes the pellet temperature to reach the melting temperature of the material mixture of the pellet. Therefore, with tolerances this tight, COMSOL was chosen as the analysis tool for this task due the accuracies provided by the finite element method and tools provided by COMSOL for geometry and mesh creation.

This conference paper is not of sufficient size to provide all the details of the equations involved in creating gas-gap conductances. The equations provided by Madhusudana[3] were followed precisely in implementing this COMSOL model. It is sufficient to state here that a fully-nonlinear representation for the gas-gap size, pressure feedback upon the gas-gap conductance as the surfaces touch, and gas-jump condition are all fully coupled into the model. In addition, the degradation in both gas thermal conductivity and gas-jump condition are also conservatively estimated based on the release of fission gas from the pellet into the helium environment. COMSOL easily allows input of these complexities quite well through the graphical user interface, but did result in a highly-nonlinear solution process. Indeed, the inclusion of the gas-gap conductance through the thin-film resistance feature of the COMSOL heat transfer module is quite impressive. It is almost as if COMSOL were developed precisely to be able to solve a problem of this type.

## 6 Defining the Correct Nuclear Heating and Boundary Conditions

Recall that the thin-film resistance boundary conditions also allow for the elimination of the need to mesh these thin regions. In addition to the complex boundary conditions coupled through the thin-film resistance feature, several other boundary conditions were also enabled into the model. On the external capsule surfaces, the bottom and top surfaces are set to the natural boundary condition provided by the insulated boundary of COMSOL. The side walls of the capsule housing are set to the COMSOL-provided convection boundary condition at the HFIR-specific coolant flow rate and temperature designed for this test capsule within HFIR. Upon researching this type of COMSOL boundary condition, it was realized that it is identical to the classical Sieder-Tate correlation[6] for convection heat transfer coefficient. Within the capsule, if a boundary is not specified as a thin-film resistance, then it is assumed to be a continuous heat transfer internal boundary to the model. For example, both the spring and screw (304-SS) will need to remove their heat by conduction to the surrounding helium gas.

The surfaces defined by the cut created by the $\frac{1}{4}$ "pie slice" of the capsule is assumed to be symmetric (analagous to an axi-symmetric assumption in 2D). In order to provide for maximum versatility, it was initially desired to produce a full 3D representation of the capsule. However, difficulties in constraining the pellet structurally required the creation of a symmetry boundary condition. Several 3D constraints on the pellet itself were attempted, but, in the end, it was realized that this single constraint was causing the results to be tainted and inconsistent.

The structural mechanics portion of the model assumes that the bottom of the lower heat sink will be constrained in the axial direction. The top of the pellet is set to receive a "load" boundary condition from the compressed spring force and the weight of the metal masses above the pellet. The "pie slice" symmetry constraint was assumed for all the structures in the model. In particular, this symmetry constraint was necessary for the pellet structural mechanics to be stable and produce reliable results.

A separate nuclear physics calculation was performed to estimate the heat generation for all the metal parts in the model. The pellet itself is a fissile material, so the maximum heat generation in the model is received in this domain.

## 7 Solver Experience

The base model, because it was 3D, required a modest level of resources in order to solve. Our Linux cluster is built with large memory compute nodes (presently 64 GB RAM per node), so that a reasonably-sized heat conduction problem (T), coupled with 3-component structural mechanics displacement field (u,v,w), and contact-surface pres-

sure field (Tn) can be readily solved. Indeed, the quadratic-basis extra-coarse and coarser mesh cases could be comfortably solved in fully-coupled mode using the direct solver within a single 64GB compute node. Even the more-demanding coarse and normal mesh cases could still be readily solved either by segregating the solution space, or allowing for a 2-3 compute node distributed-parallel solver sequence. Test problems were conducted from $\approx$ .03 to $\approx$ 2.3 Mdof to examine solution consistency and accuracy. It was found that the quadratic-basis, extra-coarse mesh ($\approx$ 0.22 Mdof) was a sufficient level of shape-function order and mesh density. It was also determined that attempts to split the problem into smaller pieces to gain speed using a segregated solution approach was not a wise choice for this problem. On the contrary, it was determined that a fully-implicit (1.0) damping, fully coupled, direct solver was essentially required for this tightly-coupled nonlinear problem. The new double-dogleg solver in v4.3 was briefly investigated, but no conclusions have been obtained. The parametric sweep capability was heavily utilized to investigate several different power levels. Attempts to further automate by parametric sweeping multiple parameters (such as gap size, pellet thermal conductivity, etc.) did not function as expected in a distributed-parallel batch-mode operation. Therefore, it was kept simple by a single-parameter sweeping operation on power level. The user interface, multiple solution storage, restart capability, results display, etc., all worked beautifully and allowed efficient use of time and resources.

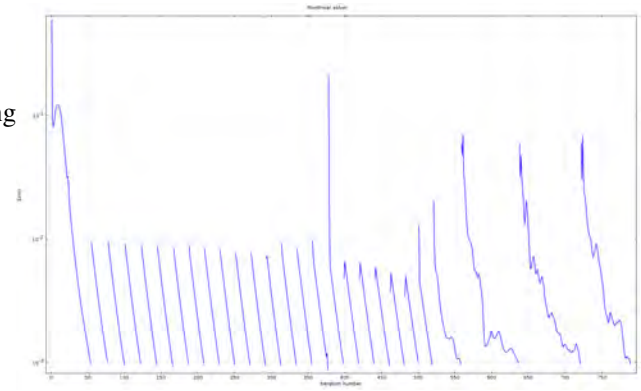

**Fig. 2** Iteration Sequence for Typical Design-Basis Results. Each convergence curve represents a 5% increment in reactor power starting at zero (left) to 130% (right) power. The pellet is pressing against the side wall starting at 115% power.

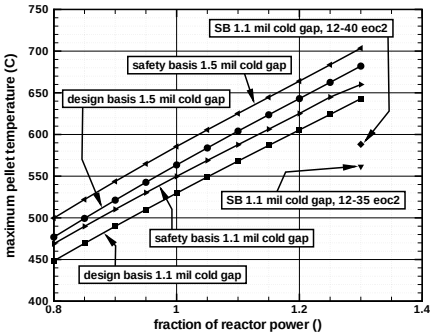


**Fig. 3** Maximum Pellet Temperature as a Function of Fractional Reactor Power and Initial Cold Radial Gap Size.

## 8 Solutions and Results

A typical plot of the convergence curves for parametric sweeps of an earlier design is shown in Fig. 2. The first iteration, at zero power and inlet temperature, takes a significant number of iterations to satisfy the initial gap size corresponding to the pellet thermal expansion from room temperature and the effect of the spring load on the pellet. Thereafter until the fractional power is about 1.10, the convergence rate is quite stable and essentially the same for all power fraction values. Then starting at a fractional power of 1.15, the pellet side starts to touch the adjacent heat sink in a significant manner. When this occurs, the solution becomes much more nonlinear and difficult to solve. Nevertheless, the solution did converge to a residual value below 0.001 for all variables in a reasonable amount of time.

Several curves of maximum pellet temperature as a function of fractional power level corresponding to a 1.1 mil and 1.5 mil initial cold radial gaps on the side of the pellet are shown in Fig. 3. Note that typically a curve of this type might experience more gradual downturn due to the effect of thermal conductivity change as a function of temperature. However, in this case, the pellet thermal conductivity has been assumed constant, and therefore, any downturn is due to the non-pellet materials in the model. In addition to the design-basis curves, a second set of safety-basis curves for both the 1.1 mil and 1.5 mil cold gaps are overlaid upon Fig. 3 . The safety-basis curves are evaluated at a fractional power level of 0.8 up to either 1.3 or above the melting temperature of 650 °C whichever occurs first.

Fig. 4 shows the corresponding average gap size (mils) for both the 1.1 and 1.5 mil initial cold gap along the pellet side wall. As in Fig. 3, the safety-basis power fraction sweeps are also added to Fig. 4. A similar change in slope of these curves is also seen when the pellet approaches the side wall. It is not obvious that any of these curves indicate that the wall is touched by the pellet. Note that the average gap sizes do not completely approach zero because there is a curvature in the pellet side wall as a result of the thermal expansion growth shape.

Fig. 5 provides an overall capsule temperature slice for the design-basis case at 100% power. Note that the hottest two regions are about the pellet and screw/spring region, while essentially all the other regions are dramatically lower in temperature (blue color). There is a slightly lighter blue region right around the pellet indicating a sig-

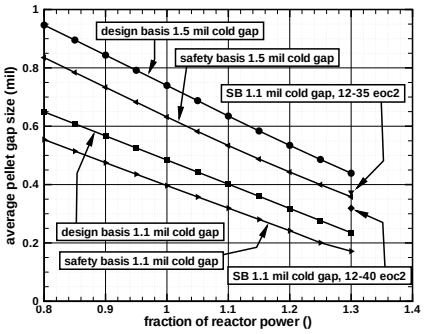


**Fig. 4** Average PelletSide (Radial) Gap Size as a Function of Fractional Reactor Power and Initial Cold Radial Gap Size.

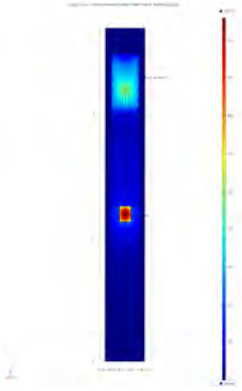

**Fig. 5** Temperature Slice (°C) for the Design Basis Case at 100% Power. The bare-pellet is shown as the hottest region, and the helium-enclosed region about the spring is also highlighted.

nificant level heat transfer into the heat-sink domains (a design feature).

A close up of the screw and spring domain for the safety-basis case at 130% power is given by Fig. 6. The 3D aspect to the problem is shown by Fig. 6, and it indicates that the screw and spring are adequately cooled within the helium-filled domain of the capsule.

The effect of thermal expansion growth in the safety-basis results is given by Fig. 7 for the 1X exaggeration in the deformed displacement. Similarly, Fig. 8 shows a 100X exaggeration of the same pellet result as Fig. 7 from a side view. One can visualize the expanded shape on all sides of the pellet, but particularly on the side walls which are unconstrained prior to touching the adjacent side walls.

The average gap size is shown in Fig. 9 for the design basis case at 100% power. The corresponding safety-basis case has a much smaller average gap size than the design-basis case. As the pellet continues to heat-up with increasing power level, the side walls will eventually touch and cause the side-gap surface pressure to touch and eventually close completely. A typical result of partial gap closure is shown by the imposed pressure distribution in Fig 10 for the safety-basis case. Note that the design-basis

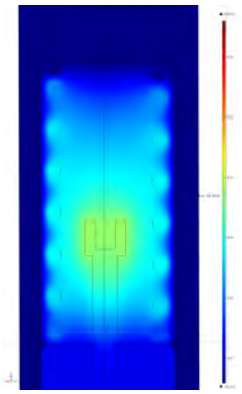

**Fig. 6** Temperature Contour of the $\frac{1}{4}$ Pie Slice Modeled Volume of the Screw and Spring Domains for the 1.1mil Cold-Gap Safety-Basis Conditions at 130% Power.

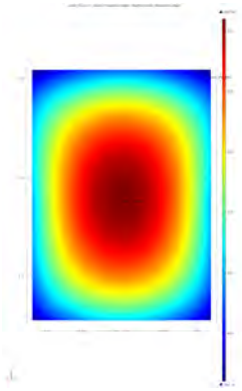

**Fig. 7** Temperature Contour with Thermal-Expansion Deformation Visualization Enabled at 1X, Along the $\frac{1}{4}$ Pie Slice Surface of the Pellet Domain for the 1.1 mil Cold-Gap Safety-Basis Conditions at 130% Power.

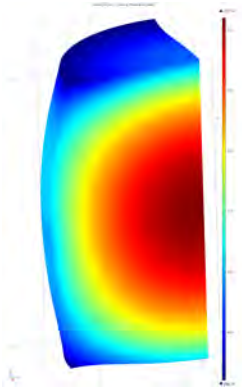

**Fig. 8** Temperature Contour with Thermal-Expansion Deformation Visualization Enabled at 100X, Along the $\frac{1}{4}$ Pie Slice Surface of the Pellet Domain for the 1.1 mil Cold-Gap Safety-Basis Conditions at 130% Power.

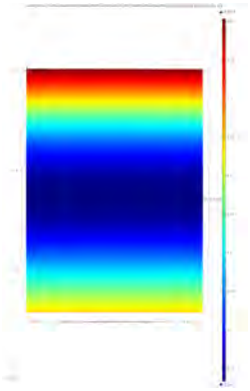

**Fig. 9** Average Pellet Side Gap Size (mils) for the 1.1 Mil Cold-Gap Design-Basis Conditions at 100% Power.

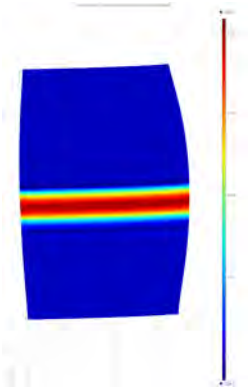

**Fig. 10** Average Pellet Side Gap Imposed Pressure for the 1.1 Mil Cold-Gap Safety-Basis Conditions at 130% Power, shown at 100X deformed view.

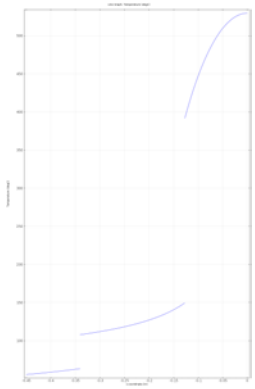

**Fig. 11** Temperature Cut Line in the Radial Direction at the elevation of Maximum Temperature. The large step-changes correspond to the gas-gap locations.

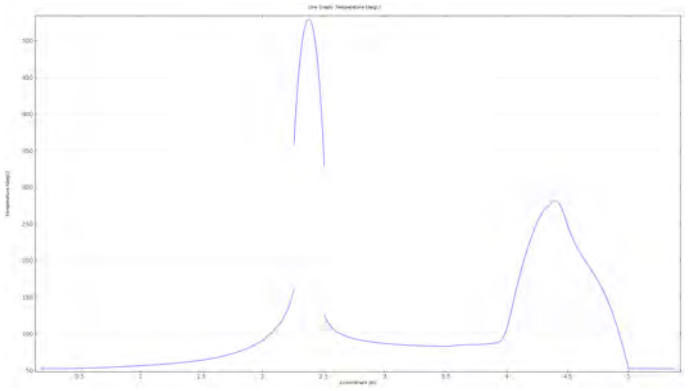

**Fig. 12** Temperature Cut Line in the Axial Direction at the Capsule Centerline.

case does not touch, hence, shows no pressure inside the gap space. On the other hand, the safety-basis case shows only a relatively narrow region of actual pellet touching the side walls as seen by the yellow and red band around the pellet side wall.

A mid-segment X-Y-axis cut line was formed in the COMSOL results section to visualize the temperature profile at the point of maximum pellet temperature as shown in Fig. 11. Note the large change in temperature across the gas gap between the pellet and lower heat sink, and a smaller change in temperature across the gas gap between the lower heat sink and the capsule housing. For this quadratic-basis design-basis solution, the temperature profile shows clear curved response due to the heat generation in the pellet region.

A Z-axis cut line was formed along the capsule centerline in order to visualize the maximum temperature changes across the entire device. By examining the results in this manner, one can visualize how the heat flux crosses the lower heat sink and upper heat sink from both the pellet and the screw-pellet helium-flooded region. Fig. 12 shows these temperature profiles for the design-basis case. From this perspective, the reader can visualize an asymmetry aspect of the solution across the axial direction due to the different materials involved. Further, the impact of the adiabatic boundary condition on the capsule ends is also captured.

An X-Y cut plane is formed at the point of maximum pellet temperature as shown by Fig. 13 for the design-basis case. Note the gas-gap effective step-change is larger between the pellet and lower heat sink than between the lower heat sink and the capsule housing outside wall. This gas-gap temperature change becomes smaller when the pellet touches the side wall (not shown).

A similar X-Y cut plane is formed at the point of maximum screw temperature as shown by Fig. 14 for the design-basis case. The asymmetry and coarseness of the mesh in the screw and spring region is revealed by Fig. 14. An important feature about this portion of the model is that since there is no physical contact by solid surfaces, the heat generation in the SS-304 screw and spring parts is removed entirely by conduction through the helium and fission-gas fluids.

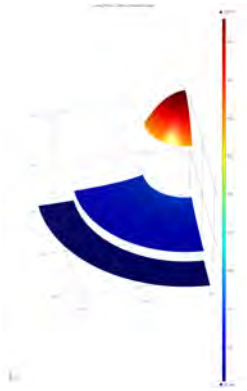

**Fig. 13** Temperature Height-Enabled Profile Along a X-Y Cut Plane at the Point of Maximum Pellet Temperature for the 1.1 Mil Cold-Gap Design-Basis Conditions at 100% Power

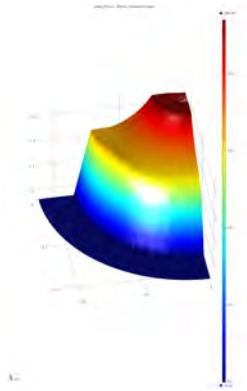

**Fig. 14** Temperature Height-Enabled Profile Along a X-Y Cut Plane at the Point of Maximum Screw Temperature for the 1.1 Mil Cold-Gap Design-Basis Conditions at 100% Power.

## 9 Nuclear Quality-Assurance Requirements

In order to perform nuclear-safety related calculations for HFIR applications at ORNL for the DOE, the computer codes used must be qualified through an existing software quality assurance program. A previous COMSOL conference paper[7] has presented how the SQA process was performed for COMSOL v3.5a. This project enabled a similar process to qualify v4.2a, and v4.3 is expected to be qualified in the near future.

In addition to the code software qualifications, the calculations themselves must be formally documented in a thorough and complete manner. The original work must be formally checked, reviewed, and independently reviewed. The present work was reviewed against both a separate $r-z$ COMSOL model produced in 2D axi-symmetric, and independently-reviewed against a similar ANSYS model. In general, both the 2D COMSOL and ANSYS models produced similar results that were slightly lower in temperature than the present 3D model described herein. It is not clear why that difference exists, but it is also known that the present 3D model is complete out to the ends of the capsule housing, whereas, certain simplifications were incorporated into the companion 2D models.

## 10 Conclusions

Through the model briefly described and results presented herein, the COMSOL code has played an important early role toward the production of Pu-238 at the ORNL HFIR for NASA. Exclusive of the nuclear physics, all aspects of the thermal-structural interaction physics have been captured by the COMSOL models developed. Upcoming post-irradiation examinations may soon disclose how well COMSOL has performed in this regard. It anticipated that COMSOL will continue to contribute toward the success of the production of Pu-238 at HFIR for NASA.

**Acknowledgements** The authors would like to acknowledge and thank Drs. Mian Qin and Jinlan Huang, both of COMSOL tech support, for their valuable insight and suggestions; particularly on the structural mechanics coupling to this analysis.

## References

1. "Plutonium 238 Production Project," `http://www.ne.doe.gov/pdfFiles/factSheets/2012_Pu-238_Factsheet_final.pdf`, February 15, 2011, The U.S. Department of Energy's Office of Nuclear Energy.
2. Munger, F., "Twenty Million Plutonium Pilot Project at ORNL," `http://blogs.knoxnews.com/munger/2012/03/plutonium-project-at-ornl.html`, March 22, 2012, Knoxville News Sentinel, Atomic City Underground Blog.
3. Madhusudana, C., *Thermal Contact Conductance*, Springer-Verlag, Inc., New York, 1996.
4. "AECO Information Modeling and CAD Production Software," `http://www.bentley.com/en-US/Products/microstation+product+line/`.
5. "Thermophysical Properties of Matter Database," `https://cindasdata.com/Applications/TPMDDEMO/splashScreen`, 2010-2011, CINDAS LLC Database, Data compiled by Center for Information and Numerical Data Analysis and Synthesis at Purdue University.
6. Sieder, E. N. and Tate, F. E., "Heat Transfer and Pressure Drop in Tubes," *Ind. Eng. Chem.*, Vol. 28, 1936, pp. 1429–1436.
7. Freels, J. D., "Implementation of Oak Ridge National Laboratory Software Quality Assurance Requirements for COMSOL 3.4," *COMSOL Conference CD*, COMSOL Conference Boston 2008, October 2008.